

# Does Interpretability of Neural Networks Imply Adversarial Robustness?

Adam Noack  
University of Oregon  
Eugene, OR  
anoack2@uoregon.edu

Isaac Ahern  
University of Oregon  
Eugene, OR  
iahern@uoregon.edu

Dejing Dou  
University of Oregon  
Eugene, OR  
dou@cs.uoregon.edu

Boyang Li  
Baidu Research  
Sunnyvale, CA  
boyangli@baidu.com

## Abstract

*The success of deep neural networks is clouded by two issues that largely remain open to this day: the abundance of adversarial attacks that fool neural networks with small perturbations and the lack of interpretation for the predictions they make. Empirical evidence in the literature as well as theoretical analysis on simple models suggest these two seemingly disparate issues may actually be connected, as robust models tend to be more interpretable than non-robust models. In this paper, we provide evidence for the claim that this relationship is bidirectional. Viz., models that are forced to have interpretable gradients are more robust to adversarial examples than models trained in a standard manner. With further analysis and experiments, we identify two factors behind this phenomenon, namely the suppression of the gradient and the selective use of features guided by high-quality interpretations, which explain model behaviors under various regularization and target interpretation settings.*

## 1. Introduction

Deep neural networks (DNNs) have produced unprecedented results across a wide range of tasks. However, their impressive performance has been clouded by two widely known weaknesses, namely their susceptibility to adversarial input perturbations and a lack of interpretability of their internal working mechanisms. These weaknesses erode users' trust in DNNs and limit their adoption in mission-critical applications. In this paper, we investigate the connections between the two seemingly disparate issues.

Adversarial perturbations are small, often imperceptible changes to an input that cause erroneous predictions even in state-of-the-art models [41]. Moreover, perturbations that fool one model can often fool a second, independently trained model. Many methods to find these perturbations have been developed recently such as the fast gradient sign method (FGSM) [14], projected gradient descent (PGD) [23], DeepFool [26], and the Carlini-Wagner attack

[5]. In response to these attacks, empirical defense techniques have been proposed, including adversarial training [14], defensive distillation [31], and gradient regularization [33, 10, 28, 18]. Despite active research [13, 34, 4, 27, 17], the reason for the existence of adversarial perturbations remains a debated topic.

A second weakness of DNNs is the difficulty of understanding how a DNN reaches its predictions. This is especially undesirable in domains such as medicine and law where the reasoning behind a decision is just as important as the decision itself. The necessity of DNN interpretability has led to the creation of a sizeable corpus on explaining the predictions that includes techniques such as simple gradient [3], SmoothGrad [37], DeepLIFT [36], Integrated Gradients [40], and LIME [32]. While interpretation-generating mechanisms help reduce the complexity of DNN behavior, by and large DNNs remain opaque.

Interestingly, recent results suggest that the two apparently separate issues of brittleness and uninterpretability are connected. Specifically, several works demonstrated that robust networks trained to defend against adversarial attacks also tend to be interpretable. Tsipras et al. [43] found that the gradients of the loss function with respect to the input for adversarially trained networks align well with what humans find important. Similarly, it has been noticed that gradient regularization [33] and a Lipschitz constraint [11] both lead to qualitatively interpretable gradient maps. Etman et al. [11] showed that the gradients of Lipschitz regularized DNNs also align closely with the input image.

With this paper, we set out to investigate the converse question: *if we train a network to have interpretable gradients, will it be robust against adversarial attacks?* In our experiments, we train a model to match the interpretations generated from a robust model acquired via adversarial training, which provides interpretations that are more human-like than non-robust models. We call this method interpretation regularization. The newly trained model is then shown to be equally or more robust than Jacobian regularization with more constraints.

With these experimental results, the answer to the ques-

tion appears to be yes. Through further analysis, we discover that two factors contribute to the effectiveness of interpretation regularization: the suppression of the gradient and the selective use of features guided by high-quality interpretations. The two factors can explain model behaviors under various settings of regularization and target interpretation.

With this paper, we make the following contributions:

- We empirically investigate if the interpretability of deep neural networks implies robustness against adversarial attacks. We find that simply requiring the model to match interpretations extracted from a robust model can improve robustness.
- To explain the experimental results, we analyze the connection between Jacobian regularization and interpretation regularization. We identify two factors, the suppression of the gradient and the selective use of features guided by high-quality interpretations, that contribute to the effectiveness of interpretation regularization and explain model behaviors.

## 2. Related Work

### 2.1. Adversarial Attacks and Defenses

We first review relevant literature on adversarial attacks, followed by works on defenses. Szegedy et al. [41] first brought to light the brittleness of deep neural networks by finding small, imperceptible perturbations that, when added to an input sample, result in misclassification from state-of-the-art networks. In addition, they showed that the troublesome perturbations were not random; attacks designed for one network were effective when transferred to another network.

Since their discovery, various techniques have been developed to find adversarial perturbations. In [14], Goodfellow et al. introduced the FGSM for efficiently finding adversarial examples from a candidate point. FGSM first finds the sign of the gradient of the loss function and then adds the sign vector, scaled by a small amount  $\epsilon$ , to the initial image. Projected Gradient Descent (PGD) [23] works similarly but is iterative. It is common to start the attack from some random initial position near a candidate point, and then after each step, the current perturbation is projected back into the set of allowed perturbations. As with many attacks, the set of allowed perturbations is constrained by an  $\ell_0$ ,  $\ell_2$ , or  $\ell_\infty$  distance. PGD is a universal first-order adversary in that robustness against PGD adversaries implies robustness to all other first-order adversaries. The Jacobian-based Saliency Map Attack [30] (JSMA) uses the Jacobian of the function learned by a DNN to find adversarial perturbations that modify a small fraction of the input dimensions that nevertheless fool the DNN. DeepFool [26] attempts to

find the smallest perturbation needed to change the prediction of the classifier. Carlini and Wagner created three new attacks for the  $\ell_0$ ,  $\ell_2$ , and  $\ell_\infty$  metrics that produce imperceptible perturbations to fool the target network [5].

Attacks can be characterized in a few ways. The above attacks are considered white-box because they require access to the gradient of the model’s loss function. Intriguingly, Papernot et al. showed that effective attacks could be created even if the original model’s gradients were not available [29]. In this paper, however, we focus our attention on white-box attacks as they are stronger than black-box attacks [23]. In addition to the white-box / black-box dichotomy, adversarial attacks can also be classified as either untargeted or targeted. Untargeted attacks work by adjusting the input sample so that the loss is maximized but they do not attempt to force a certain prediction. On the other hand, targeted attacks *do* attempt to perturb the input in a way so that a target class’s score function is maximized.

In response to the existence of adversarial examples and the growing number of methods to quickly find them, a variety of defenses have been introduced. In [14], Goodfellow et al. introduce adversarial training as a defense against FGSM perturbations. Adversarial training involves placing the adversary in the training loop where it perturbs each training sample before it is passed through the model. In doing this, the hope is the DNN can adjust its parameters to withstand the worst case perturbations [14, 23]. In practice, adversarial training has been shown to be the best defense in many cases.

Born out of the realization that adversaries often use noisy and extreme gradients to find adversarial examples, a class of techniques that regularize the gradients of the network in some manner has emerged. Ross et al. [33] take the idea of double backpropagation [10] and modify it for a cross-entropy loss function. They show that regularizing the gradient of the loss with respect to the input is an effective defense against FGSM, JSMA, and the targeted gradient sign method [21]. In a similar vein, Jakobovitz et al. [18] showed that networks trained to regularize the gradient of each output logit with respect to the input (i.e. the Frobenius norm of the input-output Jacobian) are robust to FGSM, JSMA, and DeepFool attacks. They also provide evidence that regularizing the size of the input-output gradients reduces the positive curvature of the decision boundary, and the reduction of this positive curvature is correlated with increased robustness [25]. In addition to improving adversarial robustness, Jacobian regularization has been shown to be beneficial to generalization [38].

Unfortunately, the computational costs associated with Jacobian regularization scale linearly with the number of output classes, so in the past, Jacobian regularization has not always been a computationally feasible defense for classification problems with large output spaces. Recently,

however, Hoffman et al. proved that one can quickly approximate the true value of the Frobenius norm of the Jacobian [16]. This method has the potential to make Jacobian regularization quite easy and efficient to implement, even when the output space is large.

In addition to these defenses, others have been proposed. Defensive Distillation [31] trains a small network to match the output values generated from a larger network; this results in the small network being robust to some attacks. Parseval Networks, which [6] constrain the Lipschitz constant of each hidden layer of a DNN to be small, and networks trained with Cross-Lipschitz regularization [15], which forces the differences between gradients of each class score function to be small, give robustness in certain regions around datapoints.

## 2.2. Interpreting DNNs

In the contemporary literature, the problem of interpreting DNNs has narrowed in on the more concrete subproblem of interpreting the model predictions. The typical form these interpretations take are an estimation of the degree to which each input feature contributes to a given prediction; this type of interpretation is often referred to as an *importance* or *attribution* or *sensitivity* or *saliency* map. A number of techniques exist for computing saliency maps for a model. The naive approach of linearly approximating the model local to the desired prediction  $(\mathbf{x}, f(\mathbf{x}))$  via the tangent plane

$$f(\mathbf{x} + \boldsymbol{\varepsilon}) = f(\mathbf{x}) + \nabla f(\mathbf{x})^\top \boldsymbol{\varepsilon} + o(\boldsymbol{\varepsilon}^\top \boldsymbol{\varepsilon}) \quad (1)$$

provides a high degree of interpretability in terms of the simplicity of the approximation and the meaning of the weights:  $|\frac{\partial f(\mathbf{x})}{\partial x_i}|$  is the relative importance of the feature  $x_i$ . For classification models where  $f$  outputs the class probability distribution, the weights  $\nabla f(\mathbf{x})$  can be interpreted roughly as a rule that, local to  $\mathbf{x}$ , a change in  $x_i$  by  $\pm \varepsilon$  corresponds to a change of  $\pm \varepsilon \frac{\partial f(\mathbf{x}_0)}{\partial x_i}$  in the certainty of the class label. Furthermore, these saliency maps are readily visualized on image data by activating the input pixels according to their relative importance scores.

While such interpretations empirically often highlight salient features of an image, under the standard supervised training paradigm, DNN gradient saliency maps suffer from a large degree of visual noise. It is sometimes difficult to ascertain to what degree these maps visually align with a human’s evaluation of importance, and to what extent this noise reflects certain underlying properties of the classification network. This has motivated the development of more elaborate saliency map techniques in order to tease out more structured and visually meaningful, but perhaps less locally faithful, interpretations.

Due to the recent attention that model interpretability has received, many interpretation mechanisms have

been proposed. Some commonly considered interpretation-generating methods include: the simple gradient method described above [3], Gradient  $\times$  Input [36], probabilistic noise-based techniques like SmoothGrad [37] and VarGrad [1] which approximates respectively the mean and variance saliency maps about the prediction of interest given small random-noise perturbed input. Integrated Gradients [40] computes saliency as the path integral of the gradients along the straight line path from a baseline (such as a blank image) to the desired input. Deep Taylor Decomposition [24] models the saliency in terms of the first-order Taylor approximation as with simple gradient, but expands this about an appropriately chosen point such that the attribution is performed in terms of an input-weighted gradient. DeepLIFT [36], Guided Backpropagation [39], and GradCAM / Guided GradCAM [35], are methods that backpropagate attributions of the output to the input. LIME [32] fits an interpretable local model based off binarized variables where the coefficients measure the correlations of variable activation and the model prediction. SHAP [22] computes interpretations in terms of weighted Shapley Scores approximating the performance drop when a feature is removed. In contrast to the above techniques, which focus on the present input, contrastive explanations [7] identify components that are absent in the input and contribute to the prediction.

Recent literature has focused on evaluating the appropriateness of proposed saliency maps. [20] analyzes behaviors of interpretation methods acting on simple linear models. [1] proposes that saliency methods should satisfy include sensitivity towards model and label perturbation. [19] argues they should have invariance towards uniform mean shifts of the input. Several popular methods, including Integrated Gradients, Grad  $\times$  Input, Integrated Gradients SmoothGrad (applies SmoothGrad averaging to Integrated Gradients interpretations), Guided Backprop, and Guided GradCAM, do not satisfy these apparently reasonable requirements.

## 2.3. Relationship Between Adversarial Robustness and Interpretability

Recently, it has been observed that robust networks tended to be more “interpretable”. Anil et al.[2] remark that networks trained with Lipschitz constraints have gradients that appear more interpretable. Similarly, Ross et al. [33] found that gradient regularized networks have qualitatively more interpretable gradient maps. Tsipras et al. [43] note that the simple gradient saliency maps generated from adversarially trained models are more coherent than those generated from models that are not robust to certain adversarial perturbations. They go on to hypothesize that models that achieve a small loss on adversarial examples have necessarily learned to rely on features that are invariant to the adversary’s perturbations. Because humans are natu-

rally invariant to these perturbations, robust models tend to function more similarly to the human vision system than non-robust models.

Etmann et al. [11] and Ilyas et al. [17] provide theoretical justification that robust linear and piece-wise linear classifiers tend to have gradients that are (nearly) co-linear with the input images, which are considered to introduce interpretability. Taken together, there is now converging evidence that indicates model robustness improves model interpretability. However, it is not obvious, from these discussions, whether or not making a model interpretable could improve its robustness.

A few works explored the relation between model robustness and interpretability from different perspectives than ours. [9] interpreted the role of individual neurons with adversarial examples. [12] showed that interpretations of neural networks are not immune from adversarial attacks.

### 3. Approach

The objective of our experiments is to determine if, by forcing a model to be interpretable, we can gain robustness to adversarial perturbations. To this end, we adopt a loss function that encourages the simple gradient salience map for each data point to agree with an interpretable target salience map.

We employ the following notations. A data point, drawn from the data distribution  $D$ , consists of an input  $\mathbf{x} \in \mathbb{R}^D$  and a label  $\mathbf{y} \in \mathbb{R}^K$ . Here  $\mathbf{y}$  is a  $K$ -dimensional one-hot vector, which contains a single 1 at the correct class index and zeros at the other  $K - 1$  positions. We denote the correct label index of  $\mathbf{x}$  as  $c(\mathbf{x})$ . The neural network model is denoted by  $f_{\theta}(\cdot)$ , where  $\theta$  represents the model parameters. The model’s prediction is denoted by  $\hat{\mathbf{y}} = f_{\theta}(\mathbf{x})$ . The Jacobian matrix is  $\mathcal{J}(\mathbf{x}) = \frac{\partial \hat{\mathbf{y}}}{\partial \mathbf{x}}$ . If we focus on the correct label, we can extract the simple gradient salience map as a slice of the Jacobian  $\mathcal{J}_{c(\mathbf{x})}(\mathbf{x}) = \frac{\partial \hat{y}_{c(\mathbf{x})}}{\partial \mathbf{x}}$ .

In standard training, the optimal parameters  $\theta^*$  are found by minimizing the cross-entropy loss.

$$\mathcal{L}_{XE}(\mathbf{x}, \mathbf{y}, \theta) = \sum_i y_i \log \hat{y}_i = y_{c(\mathbf{x})} \log \hat{y}_{c(\mathbf{x})} \quad (2)$$

Assuming the availability of a target interpretation  $I(\mathbf{x})$  (covered in Section 3.1), we can add a regularization term to the standard loss in order to penalize the difference between the target salience map and the Jacobian salience map generated by the model.

$$\mathcal{L}(\theta) = \mathbb{E}_{(\mathbf{x}, \mathbf{y}) \sim D} [\mathcal{L}_{XE}(\mathbf{x}, \mathbf{y}, \theta) + \lambda \|I(\mathbf{x}) - \mathcal{J}_{c(\mathbf{x})}(\mathbf{x})\|_2] \quad (3)$$

where  $\lambda$  is a hyperparameter that controls the strength of the regularization. We optimize the above loss function using standard stochastic gradient descent (SGD) with momentum.

### 3.1. Generating Target Interpretations

Using the SmoothGrad method [37], we extract target salience maps for each data point from a pretrained neural network (details in Section 3.2).

The SmoothGrad method first samples  $N$  points around a given input  $\mathbf{x}$  from the standard Gaussian distribution and takes the mean of the simple gradient salience maps generated for each sample. Formally, having drawn  $e_i \sim \mathcal{N}(0, \sigma^2)$ , the interpretation  $I(\mathbf{x})$  is computed as

$$I(\mathbf{x}) = \frac{1}{N} \sum_{i=1}^N |\mathcal{J}_{c(\mathbf{x})}(\mathbf{x} + e_i)| \quad (4)$$

In order to filter out small values that are usually ignored by a human observer, we threshold the target salience map with the standard deviation of the raw map. For each interpretation  $I(\mathbf{x})$ , we compute the pixel-level standard deviation  $\sigma I(\mathbf{x})$  and mean  $\bar{I}(\mathbf{x})$ . Any value in the target salience map  $I(\mathbf{x})$  less than  $\bar{I}(\mathbf{x}) + \phi \sigma I(\mathbf{x})$  is set to zero. The hyperparameter  $\phi$  determines the strength of filtering. Figure 1 contains examples of generated target interpretations. It can be observed that the thresholding operation removes the smaller components of the interpretation and retains the important parts.

We choose SmoothGrad over other interpretation methods for two reasons. First, when coupled with gradient-based interpretations it satisfies the basic sensitivity and invariance properties [1, 19] discussed in Section 2.2, which assert that the interpretation is properly sensitive to the model and data distributions. Second, from an adversarial perspective, SmoothGrad can be understood as a method for canceling out the influence of small perturbations on the interpretation, which has the effect of drawing the interpretation closer to what humans find meaningful [37].

### 3.2. Adversarial Training

We create a robust neural network using adversarial training, one of the earliest and still most empirically reliable defenses. The purpose of this model is to supply the target interpretations and serve as the upper bound for robustness in the experiments.

We adopt a PGD adversary that iteratively adds perturbations to an input sample to fool a model. Formally, we let  $\mathbf{x}_t$  denote the input after  $t$  iterations of transformation and  $\mathbf{x}_0 = \mathbf{x}$ . After each perturbation is added, the data point is projected to the nearest point within an  $\ell_2$  hypersphere with the radius  $\varepsilon$  around  $\mathbf{x}_0$ . This operation is denoted by the function  $\text{clip}_{\mathbf{x}_0, \varepsilon}(\cdot)$ . The  $\text{sign}(z)$  function maps the vector  $z$  to the element-wise sign  $\{-1, 1\}$ . The iterative optimization can be characterized as

$$\mathbf{x}_{t+1} = \text{clip}_{\mathbf{x}_0, \varepsilon}(\mathbf{x}_t + \varepsilon \text{sign}(\mathcal{L}_{XE}(\mathbf{x}_t, \mathbf{y}, \theta))), \quad (5)$$



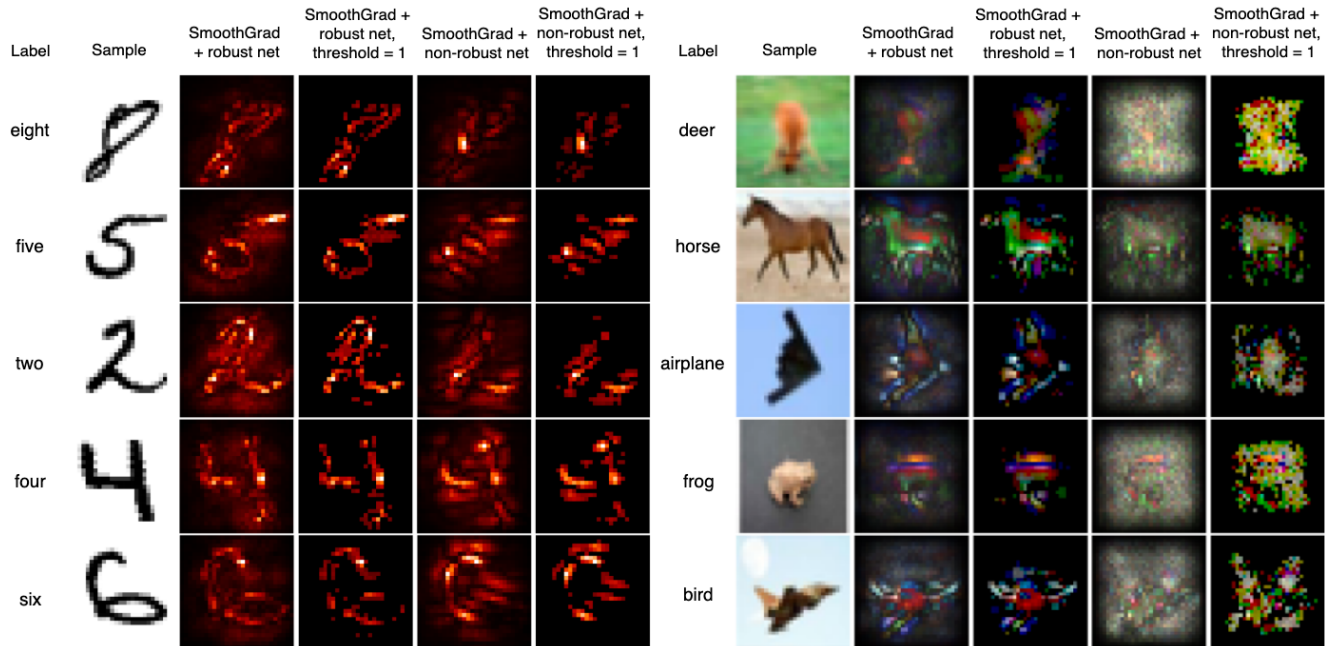


Figure 1: MNIST (left column) and CIFAR-10 (right column) saliency maps from adversarially trained networks and networks with standard training. The threshold  $\phi$  is set to 1.

$$\text{clip}_{\mathbf{x}_0, \varepsilon}(\mathbf{x}') = \begin{cases} \mathbf{x}_0 + \frac{\mathbf{x}' - \mathbf{x}_0}{\|\mathbf{x}' - \mathbf{x}_0\|_2} \varepsilon & \text{if } \|\mathbf{x}' - \mathbf{x}_0\|_2 > \varepsilon \\ \mathbf{x}' & \text{otherwise.} \end{cases} \quad (6)$$

After the adversarial examples are created, they are given the original labels and used in place of the original samples for the training of a robust model.

### 3.3. Jacobian Regularization

Jacobian regularization [18] is another adversarial defense technique, which supplements the original cross entropy loss with a regularization term.

$$\mathcal{L}(\theta) = \mathbb{E}_{(\mathbf{x}, \mathbf{y}) \sim \mathcal{D}} [\mathcal{L}_{XE}(\mathbf{x}, \mathbf{y}, \theta) + \lambda_J \|\mathcal{J}(\mathbf{x})\|_F] \quad (7)$$

where  $\|\cdot\|_F$  is the Frobenius norm and  $\lambda_J$  is a hyperparameter determining the strength of the regularization. Comparing Eq. 7 with Eq. 3, we can see the regularization term in Jacobian regularization suppresses all entries in the Jacobian matrix, whereas interpretation regularization is only concerned with one column of the Jacobian that corresponds to the correct label.

## 4. Experiments

In this section, we first discuss the setup for the two datasets, MNIST and CIFAR-10, followed by the baseline techniques. After that, we present the empirical findings and discuss their implications.

### 4.1. MNIST

For all of our experiments with the MNIST dataset, we used the convolutional neural network (CNN) architecture described here [42]. It has two convolutional layers of 32 and 64 filters. All filters are  $5 \times 5$  in size and have a stride of 1. Each convolutional layer is followed by a max-pooling layer where the kernel size is  $2 \times 2$  and the stride is 2. The output of the last pooling layer is fed into a fully-connected layer with 1024 neurons. Here dropout with probability  $p = 0.5$  is applied before the final softmax output layer consisting of 10 neurons. The output of all layers is passed through the ReLU activation function.

This network was adversarially trained with a PGD adversary (from the AdverTorch library [8]), starting from a random initial perturbation of the training data. We restricted the perturbations within an  $\ell_2$  norm of 1.5 (the pixel values for each image were in the range  $[0, 1]$ ) and set the number of iterations to 40. Tspiras et al. [43] demonstrated that these values produced networks that had interpretable simple gradient saliency maps. The network was trained using SGD with momentum set at 0.9, an initial learning rate of 0.01 that decayed by 90% every 10 epochs, and a batch size of 64.

We then used SmoothGrad with  $\sigma = 0.15$  and  $n = 50$  (these values provide a good balance between noise reduction and fidelity [37]) to generate a target interpretation for each training sample with the adversarially trained network. These target saliency maps were not normalized in any way.

Using these target interpretations generated from the robust network, we trained a new network with the same architecture with our loss (equation 3), again using SGD with momentum set at 0.9, an initial learning rate of 0.01 that decayed by 90% every 10 epochs, and a batch size of 64. We performed a grid search across  $\lambda$  (controls the strength of the regularization) and  $\phi$  (controls the target interpretation threshold) and found that a  $\lambda$  of 0.07 and a  $\phi$  of 1 produced the best results. The results of this experiment can be found in the Interp. Reg. R. row of Table 1.

We then conducted an experiment in which we took the original target interpretations from the robust network and randomly permuted their values and trained a second network to match these permuted target interpretations (row titled Interp. Reg. R. Perm. in Table 1). We used the same threshold value,  $\phi = 1$  and tuned  $\lambda$  so that the training loss was comparable to our other nets ( $\lambda = 0.05$ ). Our goal with this experiment was to determine the degree to which the distribution of values in the target interpretation mattered.

We then carried out a third experiment with our method. We extracted target interpretations using SmoothGrad from a model that was trained in a standard manner (so it had low robustness to the PGD adversary) and trained a second model to match these target interpretations (Interp. Reg. N.R.). We performed a grid search over various values of  $\phi$  and  $\lambda$ , finding  $\phi = 1$  and  $\lambda = 0.33$  to produce the best results.

In order to investigate the effects of different defenses and regularization methods, we produce a number of baselines, including standard training with only natural images (Std. Training), adversarial training with the PGD adversary described above (Adv. Training), and Jacobian regularization. All results are in Table 1.

## 4.2. CIFAR-10

For our CIFAR-10 experiments, we used a CNN with the architecture in [31]. The CNN has four convolutional layers: the first and second have 64 filters, and the third and fourth have 128 filters. Each filter has a stride of 3. After the second and fourth convolutional layers, max-pooling with a kernel size of 2 was used. The convolutional layers were followed by two fully connected layers of 256 units each before the final softmax output layer of 10 neurons. Dropout with  $p = 0.5$  was used on the fully connected layers during training. ReLU was the activation function used for all of the layers.

This architecture was then adversarially trained with a PGD adversary. Each perturbation started from a random initial position and was constrained by an  $\ell_2$  norm with epsilon at 0.314 (again, the pixel values for each image were in the range [0,1]), and again the number of iterations was set to 40. As with MNIST, Tsipras et al. [43] demonstrated that

	MNIST	
	Std. Acc.	Adv. Acc.
Std. Training	99.38 ± 0.05	61.05 ± 0.57
Adv. Training	99.29 ± 0.02	90.21 ± 0.10
Jacobian Reg.	99.13 ± 0.03	82.86 ± 0.10
Interp. Reg. R.	99.15 ± 0.02	85.17 ± 0.21
Interp. Reg. R. Perm.	99.12 ± 0.04	80.83 ± 0.34
Interp. Reg. N.R.	99.13 ± 0.05	60.96 ± 1.13

Table 1: MNIST accuracy and 95% confidence intervals for each network on the unperturbed test data (Std.) and PGD-perturbed test data (Adv.) based on  $n = 5$  independent trials.

	CIFAR-10	
	Std. Acc.	Adv. Acc.
Std. Training	78.29 ± 0.26	14.93 ± 1.49
Adv. Training	74.51 ± 0.20	57.43 ± 0.15
Jacobian Reg.	74.21 ± 0.24	51.34 ± 0.13
Interp Reg.	74.66 ± 0.25	51.43 ± 0.39

Table 2: CIFAR-10 accuracy and 95% confidence intervals for each network on the unperturbed test data (Std.) and PGD-perturbed test data (Adv.) based on  $n = 5$  independent trials.

training against this adversary produced networks with interpretable gradients. The network was trained using SGD with momentum at 0.9, an initial learning rate of 0.01 that decayed as with MNIST, and a batch size of 100.

With this robust network, we used SmoothGrad to generate the target saliency map for each input image. As with MNIST, these saliency maps were not normalized. We then used the target saliency maps to train a new network with the same architecture using our modified loss (equation 3). The network was trained using SGD with momentum at 0.9, an initial learning rate of 0.01 that decayed as with MNIST, and a batch size of 100.

Again, we performed a grid search across  $\lambda$  and  $\phi$ , finding  $\lambda = .025$  and  $\phi = 1$  to provide a training loss close to that of adversarial training. To provide baselines for comparison, we trained other copies of the architecture using standard training, adversarial training (using the same PGD adversary described above), and Jacobian regularization. Again, we tuned the hyperparameter  $\lambda_J$  for Jacobian regularization so the final training loss matched those networks trained with interpretation regularization to facilitate meaningful comparison.

	$\ \nabla f_{c(\mathbf{x})}(\mathbf{x})\ $	$\ \nabla f_{\mathbf{y}\setminus c(\mathbf{x})}(\mathbf{x})\ $
Std. Training	$7.43 \pm 0.04$	$3.93 \pm 0.02$
Adv. Training	$2.48 \pm 0.04$	$1.47 \pm 0.02$
Jacobian Reg.	$1.69 \pm 0.01$	$0.68 \pm 0.01$
Interp. Reg. R.	$1.72 \pm 0.01$	$1.19 \pm 0.01$
Interp. Reg. R. Perm.	$0.85 \pm 0.01$	$1.67 \pm 0.01$
Interp. Reg. N.R.	$5.45 \pm 0.00$	$2.37 \pm 0.02$

Table 3: Mean gradient norms on MNIST for different models. The 95% confidence intervals are computed across all training samples and across five independent training sessions using the same hyperparameters as in Table 1.

### 4.3. Results

Tables 1 and 2 reports the standard and adversarial accuracy for the models on the MNIST and CIFAR-10 datasets. The adversarial accuracies are computed using PGD-perturbed test data. With unperturbed data, standard training achieves the highest accuracy and all defense techniques slightly degrade the performance. With adversarial input, adversarial training yields the best performance as we expect. Comparing the interpretation regularization method with Jacobian regularization, the former outperforms by a margin of 2.31% on MNIST and roughly on par with the latter on CIFAR-10.

To further understand the reason behind the good performance of interpretation regularization, we compute the norm of the gradients for the correct label  $\nabla f_{c(\mathbf{x})}(\mathbf{x})$  and those of the incorrect labels, denoted as  $\nabla f_{\mathbf{y}\setminus c(\mathbf{x})}(\mathbf{x})$  on all MNIST models. We aggregated over all output logits to find the non-label gradient magnitudes and then aggregated over all of the samples in the training set. We report the mean norms over the dataset for both correct and incorrect label logit gradients. See Table 3 for the complete results.

The results show that for most models,  $\nabla f_{c(\mathbf{x})}(\mathbf{x})$  was indeed nearly twice as large as  $\nabla f_{\mathbf{y}\setminus c(\mathbf{x})}(\mathbf{x})$ . Both Jacobian regularization and interpretation regularization have low gradient norms. Adversarial training, despite being the strongest defense, has higher gradient norms than the two other defenses we tested. Interestingly, the lowest norm for  $\nabla f_{c(\mathbf{x})}(\mathbf{x})$  are achieved when the target interpretations are randomly permuted.

### 4.4. Discussion

We find it surprising that interpretation regularization performs comparably with or better than Jacobian regularization. We hypothesize two factors which explain the success, and attempt to disentangle their contributions towards this phenomenon. First, a qualitative analysis shows Jacobian regularization and interpretation regularization bear some similarities. Second, the robust target interpretation

guides the new model to focus on features which we hypothesize are robust under adversarial perturbation, and encode small gradient priors which induces interpretation regularization to suppress the magnitude of the gradient.

**Connection between Jacobian and interpretation regularization.** Jacobian regularization attaches a uniform prior for small gradients on this column. In comparison, interpretation regularization proposes a candidate distribution for the gradient. Despite these differences, we can show that these two methods bear some similarities.

Jacobian regularization forces the model to constrain the weights it learns so that the gradients  $\|\frac{\partial f(\mathbf{x})}{\partial \mathbf{x}}\|_{\mathbf{x}=\mathbf{x}_0}$  are small, smoothing out the local geometry of the loss function and pushing the decision boundary away from points that are candidate adversarial examples. Let  $\rho(\mathbf{x})$  be an upper bound on the change in confidence necessary to flip the prediction of  $f(\mathbf{x})$ , for instance, 50%. If a point  $\mathbf{x}_0$  can be adversarially attacked by a small perturbation  $\delta_{\mathbf{x}_0}$ , then  $\|f(\mathbf{x}_0 + \delta_{\mathbf{x}_0}) - f(\mathbf{x}_0)\| > \rho(\mathbf{x}_0)$ . In contrast, for most random noise perturbations  $\eta$  whose magnitude  $\|\eta\| \approx \|\delta_{\mathbf{x}_0}\|$ , we should expect  $\|f(\mathbf{x}_0 + \eta) - f(\mathbf{x}_0)\| < \zeta < \rho(\mathbf{x}_0)$  to be small. In this case, we can show that the contribution to the Jacobian is predominately from the adversarial terms along the directional derivative  $\nabla_{\delta_{\mathbf{x}_0}} f(\mathbf{x}_0) = \frac{\partial f(\mathbf{x}_0)}{\partial \mathbf{x}}^\top \delta_{\mathbf{x}_0}$ . Expanding  $f(\mathbf{x}_0 + \delta_{\mathbf{x}_0})$  and  $f(\mathbf{x}_0 + \eta)$  in terms of the first-order Taylor approximations yields norm bounds on the directional derivatives

$$\|\nabla_{\delta_{\mathbf{x}_0}} f(\mathbf{x}_0)\| \approx \rho(\mathbf{x}_0) \text{ and } \|\nabla_{\eta} f(\mathbf{x}_0)\| \lesssim \zeta, \quad (8)$$

so that

$$\begin{aligned} \|\nabla_{\delta_{\mathbf{x}_0}} f(\mathbf{x}_0)\| &\approx \rho(\mathbf{x}_0) \\ &\gtrsim \frac{\rho(\mathbf{x}_0)}{\zeta} \|\nabla_{\eta} f(\mathbf{x}_0)\|. \end{aligned} \quad (9)$$

In particular, the coefficient  $\frac{\rho(\mathbf{x}_0)}{\zeta}$  is (much) larger than one. Since the norm of the adversarial perturbation is constrained by the  $\ell_2$  norm  $\varepsilon$ , the key to a successful attack is to set up  $\delta_{\mathbf{x}_0}$  such that it selects large components of  $\frac{\partial f(\mathbf{x})}{\partial \mathbf{x}_0}$ . From this we can draw two conclusions: Jacobian regularization creates robustness because it disproportionately impacts gradient components corresponding to adversarial attack directions, and as  $\delta_{\mathbf{x}_0}$  is constrained, it follows that any entries in the Jacobian matrix that are greater than others are heavily penalized by the regularization.

Interestingly, as Table 3 shows, in most setups the gradient for the correct label is greater than that of the incorrect labels. Under small perturbations, it seems reasonable to suppose the change in confidence for the correct label dissipates across the other labels, leading to smaller gradients. Thus, the gradient of the correct label is penalized more heavily than the rest. This behavior is similar to interpretation regularization, which constrains the gradient of the

correct label but not the rest. Thus, we argue that one of the reasons for the effectiveness of interpretation regularization is that, like Jacobian regularization, it constrains the gradient in the most important places.

**The quality of the interpretation matters.** The above analysis does not include the quality of the target interpretation. However, in practice, different target interpretations result in models with very different adversarial accuracies. Models trained with robust target interpretations (Interp. Reg. R.) and *permuted* robust target interpretations (Interp. Reg. R. Perm.) have similar gradient magnitudes, but different adversarial accuracy, which can only be attributed to the differences in their target interpretation. Similarly, Jacobian regularization could be considered to have all-zero target interpretations for all output labels and its adversarial accuracy is lower than Interp. Reg. R.

Intuitively, the gradient of the model indicates the important features used by the model. [17] suggests that model brittleness is caused by the model using non-robust features in making predictions. It follows that if we can constrain the model to use only robust features, we should be able to create robust models. The examples in Figure 1 suggest a qualitative difference: the interpretations from the robust model capture the most important features but the interpretations from the non-robust model appear less appropriate, potentially misleading models. Thus, we argue that another reason interpretation regularization works is the interpretation guides the model to use the correct and possibly robust features.

**Disentangling gradient magnitude and interpretation quality.** Unexpectedly, Interp Reg. R. Perm. is able to achieve a high level of robustness despite having random target interpretations. We contend that the robustness comes from the low gradient magnitudes (see Table 3) rather than the quality of the interpretation. In contrast, even though the target interpretations used by Interp Reg. N.R. may be better than random permutation, its large gradient magnitudes result in low adversarial accuracy.

An aspect of the gradient magnitude worth recognizing is that with interpretation regularization we constrain the size of the gradients by requiring them to be similar in magnitude to the target interpretations. Interp Reg. N.R. draws the target interpretation from models with Standard Training, which has large gradient norms, whereas Interp Reg. R. Perm. draws the target interpretations from Adversarial Training, which has smaller gradient norms. This may help explain the discrepancy in adversarial accuracy between Interp Reg. R. Perm. and Interp Reg. N.R.

**Does SmoothGrad create a difference?** SmoothGrad was proposed to average out noise that appear in the gradient saliency map. In our approach, the smoothed noises become small values and get removed by the thresholding. This may focus the saliency map on robust features only, as

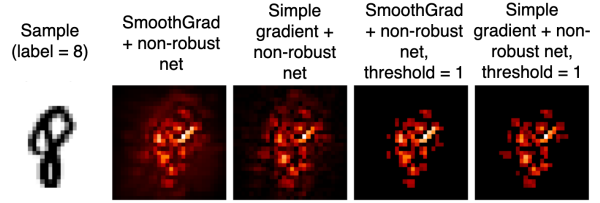


Figure 2: Comparison of original and thresholded versions of SmoothGrad and simple gradient saliency maps.

SmoothGrad highlights the important features in common over a small neighborhood. Figure 2 qualitatively compares SmoothGrad and simple gradients. The extra stroke to the left of the number eight, a potentially non-robust feature, has been assigned less importance by SmoothGrad than by simple gradient. We leave a thorough analysis of different interpretation methods for future work.

## 5. Conclusions

The abundance of adversarial attacks and the lack of interpretation of how a deep neural network makes its predictions are two issues that render many results from artificial intelligence untrustworthy in the eye of the general public. The literature suggests that these two issues may be closely related, as works have indicated qualitatively that adversarial defenses techniques, such as adversarial training [43], Jacobian regularization [33], and Lipschitz constraints [11] produce models that have saliency maps that agree with human interpretations.

These findings naturally lead to the question if the converse is true. If we force a neural network to have interpretable gradients, will it then become robust? We devise a technique called interpretation regularization, which regularizes the gradient of a model to match the target interpretation extracted from an adversarially trained robust model. Interestingly, the new model performs comparably or better than Jacobian regularization, which applies more constraints than interpretation regularization.

In the discussion, we carefully disentangle two factors that contribute to the effectiveness of interpretation regularization: the suppression of the gradient and the selective use of features guided by high-quality interpretations. With the two factors, we manage to explain model behaviors under various settings of regularization and target interpretation. We believe this study provides useful insights into the research of adversarial defenses and interpretation methods. The joint investigation of these two issues will continue to foster our understanding of deep neural networks.

## References

- [1] Julius Adebayo, Justin Gilmer, Michael Muelly, Ian J. Goodfellow, Moritz Hardt, and Been Kim. Sanity checks for saliency maps. *NIPS’18*, 1810.03292, 2018. 3, 4



- [2] Cem Anil, James Lucas, and Roger B. Grosse. Sorting out lipschitz function approximation. *ICML 2019*, 1811.05381, 2018. 3
- [3] David Baehrens, Timon Schroeter, Stefan Harmeling, Motoaki Kawanabe, Katja Hansen, and Klaus-Robert Müller. How to explain individual classification decisions. *J. Mach. Learn. Res.*, 11:1803–1831, Aug. 2010. 1, 3
- [4] Sbastien Bubeck, Eric Price, and Ilya Razenshteyn. Adversarial examples from computational constraints. *ICML 2019*, 2018. 1
- [5] Nicholas Carlini and David A. Wagner. Towards evaluating the robustness of neural networks. *CoRR*, abs/1608.04644, 2016. 1, 2
- [6] Moustapha Cisse, Piotr Bojanowski, Edouard Grave, Yann Dauphin, and Nicolas Usunier. Parseval networks: Improving robustness to adversarial examples. In Doina Precup and Yee Whye Teh, editors, *Proceedings of the 34th International Conference on Machine Learning*, volume 70 of *Proceedings of Machine Learning Research*, pages 854–863, International Convention Centre, Sydney, Australia, 06–11 Aug 2017. PMLR. 3
- [7] Amit Dhurandhar, Pin-Yu Chen, Ronny Luss, Chun-Chen Tu, Paishun Ting, Karthikeyan Shanmugam, and Payel Das. Explanations based on the missing: Towards contrastive explanations with pertinent negatives. In *Proceedings of the 32nd Conference on Neural Information Processing Systems*, 2018. 3
- [8] Gavin Weiguang Ding, Luyu Wang, and Xiaomeng Jin. AdverTorch v0.1: An adversarial robustness toolbox based on pytorch. *arXiv preprint arXiv:1902.07623*, 2019. 5
- [9] Y. Dong, H. Su, J. Zhu, and F. Bao. Towards interpretable deep neural networks by leveraging adversarial examples. *AAAI-19 Workshop on Network Interpretability for Deep Learning*, 1708.05493, 2017. 4
- [10] Harris Drucker and Yann LeCun. Double backpropagation increasing generalization performance. In *Proceedings of the International Joint Conference on Neural Networks*, pages 145–150, 1992. 1, 2
- [11] Christian Etmann, Sebastian Lunz, Peter Maass, and Carolabibiane Schnlieb. On the connection between adversarial robustness and saliency map interpretability. In *Proceedings of the International Conference on Machine Learning*, 2019. 1, 4, 8
- [12] Amirata Ghorbani, Abubakar Abid, and James Y. Zou. Interpretation of neural networks is fragile. In *AAAI*, 2017. 4
- [13] Justin Gilmer, Luke Metz, Fartash Faghri, Samuel S. Schoenholz, Maithra Raghu, Martin Wattenberg, and Ian J. Goodfellow. Adversarial spheres. In *Workshop of International Conference on Learning Representations (ICLR)*, 2018. 1
- [14] Ian Goodfellow, Jonathon Shlens, and Christian Szegedy. Explaining and harnessing adversarial examples. In *International Conference on Learning Representations*, 2015. 1, 2
- [15] Matthias Hein and Maksym Andriushchenko. Formal guarantees on the robustness of a classifier against adversarial manipulation. In I. Guyon, U. V. Luxburg, S. Bengio, H. Wallach, R. Fergus, S. Vishwanathan, and R. Garnett, editors, *Advances in Neural Information Processing Systems 30*, pages 2266–2276. Curran Associates, Inc., 2017. 3
- [16] Judy Hoffman, Daniel A. Roberts, and Sho Yaida. Robust learning with jacobian regularization. In *arXiv Preprint*, 2019. 3
- [17] Andrew Ilyas, Shibani Santurkar, Dimitris Tsipras, Logan Engstrom, Brandon Tran, and Aleksander Madry. Adversarial examples are not bugs, they are features. *NeurIPS 2019*, 2019. 1, 4, 8
- [18] Daniel Jakobovitz and Raja Giryes. Improving DNN robustness to adversarial attacks using jacobian regularization. *ECCV 2018*, abs/1803.08680, 2018. 1, 2, 5
- [19] Pieter-Jan Kindermans, Sara Hooker, Julius Adebayo, Maximilian Alber, Kristof T. Schütt, Sven Dähne, Dumitru Erhan, and Been Kim. The (Un)reliability of saliency methods. *NeurIPS Workshop 2017*, page arXiv:1711.00867, Nov 2017. 3, 4
- [20] Pieter-Jan Kindermans, Kristof T. Schtt, Maximilian Alber, Klaus-Robert Miller, Dumitru Erhan, Been Kim, and Sven Dhne. Learning how to explain neural networks: PatternNet and PatternAttribution. 2017. 3
- [21] Alexey Kurakin, Ian J. Goodfellow, and Samy Bengio. Adversarial examples in the physical world. *ICLR 2016*, 1607.02533, 2016. 2
- [22] Scott M Lundberg and Su-In Lee. A unified approach to interpreting model predictions. In *Advances in Neural Information Processing Systems 30*, pages 4765–4774. 2017. 3
- [23] Aleksander Madry, Aleksandar Makelev, Ludwig Schmidt, Dimitris Tsipras, and Adrian Vladu. Towards deep learning models resistant to adversarial attacks. *ICLR 2017*, abs/1706.06083, 2017. 1, 2
- [24] Grégoire Montavon, Wojciech Samek, and Klaus-Robert Müller. Methods for interpreting and understanding deep neural networks. *ICASSP tutorial*, 1706.07979, 2017. 3
- [25] Seyed-Mohsen Moosavi-Dezfooli, Alhussein Fawzi, Omar Fawzi, Pascal Frossard, and Stefano Soatto. Analysis of universal adversarial perturbations - published as robustness of classifiers to universal perturbations: A geometric perspective. *ICLR*, 2018. 2
- [26] Seyed-Mohsen Moosavi-Dezfooli, Alhussein Fawzi, and Pascal Frossard. Deepfool: a simple and accurate method to fool deep neural networks. *CVPR*, 2016. 1, 2
- [27] Preetum Nakkiran. Adversarial robustness may be at odds with simplicity. *ArXiv*, 2019. 1
- [28] Adam M. Oberman and Jeff Calder. Lipschitz regularized deep neural networks converge and generalize. *CoRR*, abs/1808.09540, 2018. 1
- [29] Nicolas Papernot, Patrick McDaniel, Ian Goodfellow, Somesh Jha, Z. Berkay Celik, and Ananthram Swami. Practical black-box attacks against machine learning. In *Proceedings of the 2017 ACM on Asia Conference on Computer and Communications Security*, ASIA CCS '17, pages 506–519, New York, NY, USA, 2017. ACM. 2
- [30] Nicolas Papernot, Patrick D. McDaniel, Somesh Jha, Matt Fredrikson, Z. Berkay Celik, and Ananthram Swami. The

- limitations of deep learning in adversarial settings. *IEEE European Symposium on Security and Privacy*, 2016. [2](#)
- [31] Nicolas Papernot, Patrick D. McDaniel, Xi Wu, Somesh Jha, and Ananthram Swami. Distillation as a defense to adversarial perturbations against deep neural networks. *IEEE Symposium on Security and Privacy*, 2016. [1](#), [3](#), [6](#)
- [32] Marco Túlio Ribeiro, Sameer Singh, and Carlos Guestrin. "why should I trust you?": Explaining the predictions of any classifier. *KDD*, 2016. [1](#), [3](#)
- [33] Andrew Slavin Ross and Finale Doshi-Velez. Improving the adversarial robustness and interpretability of deep neural networks by regularizing their input gradients. *AAAI*, 2018. [1](#), [2](#), [3](#), [8](#)
- [34] Ludwig Schmidt, Shibani Santurkar, Dimitris Tsipras, Kunal Talwar, and Aleksander Madry. Adversarially robust generalization requires more data. In *Advances in Neural Information Processing Systems (NeurIPS)*, 2018. [1](#)
- [35] Ramprasaath R. Selvaraju, Michael Cogswell, Abhishek Das, Ramakrishna Vedantam, Devi Parikh, and Dhruv Batra. Grad-cam: Visual explanations from deep networks via gradient-based localization. *ICCV*, 2017. [3](#)
- [36] Avanti Shrikumar, Peyton Greenside, and Anshul Kundaje. Learning important features through propagating activation differences. *ICML*, 2017. [1](#), [3](#)
- [37] Daniel Smilkov, Nikhil Thorat, Been Kim, Fernanda B. Viégas, and Martin Wattenberg. Smoothgrad: removing noise by adding noise. *ICML*, 2017. [1](#), [3](#), [4](#), [5](#)
- [38] Jure Sokolic, Raja Giryes, Guillermo Sapiro, and Miguel R. D. Rodrigues. Robust large margin deep neural networks. *IEEE Transactions on Signal Processing*, 65:4265–4280, 2016. [2](#)
- [39] Jost Tobias Springenberg, Alexey Dosovitskiy, Thomas Brox, and Martin Riedmiller. Striving for simplicity: The all convolutional net. *ICLR Workshop*, 2014. [3](#)
- [40] Mukund Sundararajan, Ankur Taly, and Qiqi Yan. Axiomatic attribution for deep networks. *ICML*, 2017. [1](#), [3](#)
- [41] Christian Szegedy, Wojciech Zaremba, Ilya Sutskever, Joan Bruna, Dumitru Erhan, Ian J. Goodfellow, and Rob Fergus. Intriguing properties of neural networks. *ICLR*, 2014. [1](#), [2](#)
- [42] TensorFlow. TensorFlow models repository, 2017. [5](#)
- [43] D. Tsipras, S. Santurkar, L. Engstrom, A. Turner, and A. Madry. Robustness May Be at Odds with Accuracy. *ICLR*, 2019. [1](#), [3](#), [5](#), [6](#), [8](#)